



The extent of fermentative transformation of phenolic compounds in the bioanode controls exoelectrogenic activity in a microbial electrolysis cell



Xiaofei Zeng^a, Maya A. Collins^a, Abhijeet P. Borole^{b, c}, Spyros G. Pavlostathis^{a, *}

^a School of Civil and Environmental Engineering, Georgia Institute of Technology, Atlanta, GA 30332-0512, United States

^b Biosciences Division, Oak Ridge National Laboratory, Oak Ridge, TN 37831, United States

^c Bredesen Center for Interdisciplinary Research and Education, The University of Tennessee, Knoxville, TN 37996, United States

ARTICLE INFO

Article history:

Received 29 July 2016

Received in revised form

21 November 2016

Accepted 23 November 2016

Available online 27 November 2016

Keywords:

Syringic acid

Vanillic acid

4-hydroxybenzoic acid

Fermentation

Exoelectrogenesis

Metabolic pathways

ABSTRACT

Phenolic compounds in hydrolysate/pyrolysate and wastewater streams produced during the pretreatment of lignocellulosic biomass for biofuel production present a significant challenge in downstream processes. Bioelectrochemical systems are increasingly recognized as an alternative technology to handle biomass-derived streams and to promote water reuse in biofuel production. Thus, a thorough understanding of the fate of phenolic compounds in bioanodes is urgently needed. The present study investigated the biotransformation of three structurally similar phenolic compounds (syringic acid, SA; vanillic acid, VA; 4-hydroxybenzoic acid, HBA), and their individual contribution to exoelectrogenesis in a microbial electrolysis cell (MEC) bioanode. Fermentation of SA resulted in the highest exoelectrogenic activity among the three compounds tested, with 50% of the electron equivalents converted to current, compared to 12 and 9% for VA and HBA, respectively. The biotransformation of SA, VA and HBA was initiated by demethylation and decarboxylation reactions common to all three compounds, resulting in their corresponding hydroxylated analogs. SA was transformed to pyrogallol (1,2,3-trihydroxybenzene), whose aromatic ring was then cleaved via a phloroglucinol pathway, resulting in acetate production, which was then used in exoelectrogenesis. In contrast, more than 80% of VA and HBA was converted to catechol (1,2-dihydroxybenzene) and phenol (hydroxybenzene) as their respective dead-end products. The persistence of catechol and phenol is explained by the fact that the phloroglucinol pathway does not apply to di- or mono-hydroxylated benzenes. Previously reported, alternative ring-cleaving pathways were either absent in the bioanode microbial community or unfavorable due to high energy-demand reactions. With the exception of acetate oxidation, all biotransformation steps in the bioanode occurred via fermentation, independently of exoelectrogenesis. Therefore, the observed exoelectrogenic activity in batch runs conducted with SA, VA and HBA was controlled by the extent of fermentative transformation of the three phenolic compounds in the bioanode, which is related to the number and position of the methoxy and hydroxyl substituents.

© 2016 Elsevier Ltd. All rights reserved.

1. Introduction

Lignocellulosic biomass is an abundant renewable source for the production of biofuels, providing an important alternative to fossil fuels. Biomass conversion to biofuels via thermochemical processes, such as hydrolysis and pyrolysis, produces streams bearing phenolic compounds, because of lignin break-down (Monlau et al.,

2014). As a result, phenolic alcohols, aldehydes, and acids are widely present in biomass-derived streams (e.g., hydrolysates, pyrolysates, and biorefinery wastewater) at concentrations ranging from milligrams per liter to several grams per liter (Ren et al., 2016; Mills et al., 2009; Borole et al., 2013). Phenolic compounds contribute to the instability and corrosiveness of pyrolysis-derived bio-oil and the observed inhibition of biomass hydrolysates to microorganisms involved in dark fermentation for H₂ and ethanol production (Jones et al., 2009; Monlau et al., 2014). Thus, phenolic compounds are regarded as a major problem in the use of biomass for biofuel production. Solvent extraction is currently practiced to

* Corresponding author.

E-mail address: spyros.pavlostathis@ce.gatech.edu (S.G. Pavlostathis).

remove phenolic compounds from hydrolysates and pyrolysates, which produces high volumes of waste streams rich in organic compounds, resulting in challenging wastewater treatment and disposal practices (Borole and Mielenz, 2011).

Microbial electrolysis cell (MEC) is a bioelectrochemical technology, which degrades organic compounds through microbial activity in the anode producing hydrogen gas (H_2) in the cathode with a small voltage input (Wang and Ren, 2013; Zhang and Angelidaki, 2014). Several studies have demonstrated significant benefits of integrating MEC technology in biofuel production. For example, MECs were studied as an alternative to or in combination with dark fermentation for enhanced H_2 production from wheat straw and corn stover hydrolysates (Lalaurette et al., 2009; Thygesen et al., 2011). A MEC was used to convert acidic and polar components of a switchgrass pyrolysate aqueous phase to renewable H_2 that can then be used in the downstream hydrogenation of bio-oil, thus reducing the need for an external H_2 supply, which is currently produced from natural gas (i.e., methane), a non-renewable fossil fuel (Lewis et al., 2015). Another potential use of MEC in biofuel production is to recycle effluent from biomass pretreatment and fermentation, thus improving water reuse in biorefineries (Borole and Mielenz, 2011).

As MEC is increasingly used with biomass-derived streams, a thorough understanding of the fate of phenolic compounds in MEC bioanodes is needed. Removal of phenolic compounds in microbial fuel cell (MFC) bioanodes has been reported in several studies (Song et al., 2014; Friman et al., 2013; Huang et al., 2011; Borole et al., 2009). Despite the reported disappearance of the parent phenolic compounds, the biotransformation extent and pathways of individual compounds were not examined in the above-mentioned studies. It is generally accepted that when the bioanode substrate is a complex organic compound, fermentation is required to convert the complex compound to mainly acetate, which can then be used in exoelectrogenesis to produce current (Kiely et al., 2011; Ren et al., 2007). Our previous studies, using a mixture of two furanic (furfural, 5-hydroxymethyl furfural) and three phenolic (syringic, vanillic, and 4-hydroxybenzoic acids) compounds, demonstrated that the phenolic compounds were not directly utilized by bioanode exoelectrogens. Instead, fermentation in the bioanode produced acetate, which was then used as an exoelectrogenic substrate (Zeng et al., 2015, 2016a). Although several phenolic metabolites were reported, the fate of the individual phenolic compounds was not elucidated, because the phenolic compounds were used as a mixture (Zeng et al., 2015). Marone et al. (2016) reported the removal of hydroxytyrosol and tyrosol from table olive brine processing wastewater treated by a bioelectrochemical system, with the detection of 3,4-dihydroxyphenyl acetic acid, 3,4-dihydroxybenzaldehyde, and *p*-hydroxyphenyl acetic acid as biotransformation products. A MFC study conducted by Hedbavna et al. (2016) showed that phenol, cresols and xylenols in groundwater were biotransformed to 4-hydroxybenzoic acid and 4-hydroxy-3-methylbenzoic acid. In this case, oxygen, nitrate, iron (III), and sulfate were present as electron acceptors in addition to the bioanode electrode.

Despite the knowledge gained from previous studies, important questions remain unanswered relative to the fate of phenolic compounds in bioanodes: (1) To what extent are these compounds transformed (e.g., aromatic rings cleaved or not)? (2) What are the biotransformation pathways? (3) Are there any limiting steps in the biotransformation pathways of these compounds in bioanodes impacting exoelectrogenic activity? To address these questions, the objective of the present study was to assess the extent of biotransformation and metabolic pathways of three phenolic compounds (syringic acid, SA; vanillic acid, VA; 4-hydroxybenzoic acid, HBA), as well as their individual contribution to

exoelectrogenesis in a MEC bioanode.

2. Material and methods

2.1. Chemicals

SA, VA and HBA were used as phenolic substrates fed in the MEC bioanode (Table 1). SA, VA and HBA have similar chemical structures, but differ in the number and position of hydroxyl ($-OH$) and methoxy ($-O-CH_3$) substituents, representing phenolic compounds derived from different lignin units (syringyl, guaiacyl and *p*-hydroxyphenyl, respectively) during the pretreatment of lignocellulosic biomass (Monlau et al., 2014). Analytical standards of 3,4-dihydroxy-5-methoxybenzoic acid (DHMB), gallic acid (GA), protocatechuic acid (PA), pyrogallol, catechol, phenol, phloroglucinol, resorcinol, and benzoic acid were used as reference for the identification of SA, VA and HBA metabolites (Supplementary Material, Table S1). All chemicals were purchased from either Sigma-Aldrich (St. Louis, MO) or Alfa Aesar (Ward Hill, MA).

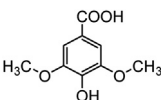
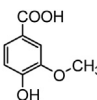
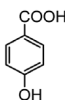
2.2. MEC

An H-type dual-chamber MEC was developed using two glass bottles (liquid volume of 200 mL for the anode and 250 mL for the cathode), an anode electrode made of a bundle of 5 stripes of carbon felt (1 cm \times 1 cm \times 5 cm, each), a cathode electrode made of platinum-coated carbon cloth (5 cm \times 6 cm), and a Nafion 117 cation exchange membrane (projected surface area of 5.7 cm²). The MEC configuration and materials were previously described in detail (Zeng et al., 2015). The anolyte was a mineral microbial growth medium consisting of the following (g/L): NH_4Cl , 0.31; KCl , 0.13; $NaH_2PO_4 \cdot H_2O$, 2.45; and Na_2HPO_4 , 4.58; along with trace metals and vitamins (pH 7.0) (Zeng et al., 2015). The catholyte was a 100 mM sodium phosphate buffer, pH 7.0. The anolyte and catholyte stock solutions were both autoclaved and deoxygenated by bubbling with N_2 for 30 min before being transferred to the MEC. A glass burette, filled with acid brine (10% $NaCl$ w/v, 2% H_2SO_4 v/v), was connected to each chamber headspace for gas collection and measurement by liquid displacement. A potentiostat (Interface 1000, Gamry Instruments, Warminster, PA) was used to set a voltage of 0.6 V at the anode against the cathode in a two-electrode setup. A reference electrode ($Ag/AgCl$, 0.199 V SHE) was inserted in the anode chamber for measuring anode and cathode potentials and conducting anode cyclic voltammetry.

Enrichment of the MEC bioanode microbial community was initiated in a MFC, using an inoculum from a different MFC anode, which had been fed with a switchgrass pyrolysis waste stream bearing levoglucosan, ketones, volatile fatty acids, as well as furanic and phenolic compounds (Lewis et al., 2015). The MFC used for enrichment in the present study was fed with a mixture of two furanic and three phenolic compounds (furfural, 5-hydroxymethylfurfural, SA, VA and HBA), as previously reported (Zeng et al., 2015). After 6 months of enrichment, a piece of MFC biofilm-attached carbon felt electrode (1 cm \times 1 cm \times 2 cm) was cut using sterile scissors and anaerobically transferred to the center of the MEC anode electrode used in the present study. The MEC bioanode was then consistently fed with the above-described mixture of furanic and phenolic compounds, maintained at room temperature (20–22 °C). During the 2-year MEC operation, the total biomass concentration in the anode chamber increased from 52.7 ± 0.9 to 352 ± 10 mg/L measured as protein, approximately 90% of which was associated with the biofilm. The MEC bioanode biofilm-associated microbial community was analyzed at 7 and 13 months of operation, following the procedure described in Supplementary Material, Text S1.

Table 1

Parent phenolic compounds used in the present study.

Parameter	Syringic acid (SA)	Vanillic acid (VA)	4-Hydroxybenzoic acid (HBA)
CAS number	530-57-4	121-34-6	99-96-7
Chemical structure			
Molecular formula	C ₉ H ₁₀ O ₅	C ₈ H ₈ O ₄	C ₇ H ₆ O ₃
Molecular weight (g/mol)	198.17	168.15	138.12
Theoretical oxygen demand (g O ₂ /g)	1.45	1.52	1.62
Electron equivalents (mol e ⁻ /mol)	36	32	28.0
G _f ⁰ (kJ/mol)	-583.95 ^a	-494.08 ^b	-416.5 ^b
pK _a ^c	3.93	4.16	4.38

^a Value from (Yaws, 2003).^b Values from (Zeng et al., 2015).^c Values from (ChemAxon).

2.3. Fermentative culture

In order to evaluate the fermentative activity in the bioanode under non-exoelectrogenic conditions, a fermentative culture was developed using an inoculum from the MEC bioanode, which had been maintained with the mixture of furanic and phenolic compounds for more than 1 year (see Section 2.2, above). Autoclaved carbon-felt (i.e., the same material as the MEC anode electrode) was placed in a 1-L glass reactor to support biofilm development. The ratio of the carbon-felt to liquid phase (1:4 v/v) was kept the same as that in the MEC bioanode. To inoculate the culture, two pieces of biofilm-attached carbon felt electrode (1 × 1 × 3 cm, each) along with 100 mL suspension removed from the MEC bioanode were anaerobically transferred to the reactor. The MEC anolyte, used as microbial growth medium, was then added to the reactor to reach a final liquid volume of 600 mL, leaving a 490 mL headspace which was filled with N₂ (ca. 0.1 bar). The culture was maintained at room temperature (20–22 °C). Weekly feedings were conducted with 1 mM SA for 1 month, a mixture of SA, VA and HBA (1 mM each) for 2 months, and then a mixture of the above-described two furanic and three phenolic compounds (0.5 mM each) for 1 month. Glucose (1 mM) was added for the first feeding only. Before each weekly feeding, 200 mL of liquid was wasted from the culture and fresh anolyte added, resulting in a hydraulic retention time of 21 d. The pH was maintained at 6.8–7.0 during each feeding cycle. CO₂ was detected in the headspace, but not H₂ or CH₄. The total biomass concentration measured as protein was 47.2 ± 1.5 mg/L, with 95% of the biomass residing on the carbon felt-attached biofilm. The biofilm-associated microbial community was analyzed at the completion of the batch runs reported in Section 2.4, below, following the procedure described in Text S1.

2.4. SA, VA, and HBA batch runs

Consecutive batch runs were conducted with SA, VA, or HBA at an initial concentration of 1 mM in both the MEC bioanode and the fermentative culture, which were developed as described in Sections 2.2 and 2.3, respectively. The headspace of the MEC and the fermentative culture were filled with N₂ (ca. 0.1 bar) at the start of each batch run. During the batch runs, the MEC anolyte and catholyte, as well as the fermentative culture, were continuously mixed magnetically. The pH, concentration of each parent compound, current and cathodic H₂ were monitored; metabolites were identified and quantified as described in Section 2.5, below. Each batch run lasted for 6 days. Between each bioanode batch run, the MEC anode chamber was drained and washed with clean anolyte to

avoid residuals being carried over to the next batch run; then fresh anolyte and catholyte added. Between each fermentative batch run, the fermentative culture was drained and washed with fresh anolyte following the same procedure as for the MEC runs, while retaining the carbon felt-attached biofilm. All 6 batch runs were repeated to confirm reproducibility.

2.5. Analytical methods

SA, VA, HBA, and acetate were analyzed and quantified using a high-performance liquid chromatography (HPLC) unit equipped with a HPX-87H column (BioRad, Hercules, CA) and a UV–vis detector at a wavelength of 210 nm, as previously described (Zeng et al., 2015). Samples were passed through 0.2 μm PTFE membrane filters before injection into the HPLC. Gas production was measured by acid brine solution displacement in glass burettes, equilibrated to 1 atm. Gas composition (H₂, CO₂ and CH₄) was quantified using a gas chromatography unit equipped with two columns and two thermal conductivity detectors, as previously described (Okutman Tas and Pavlostathis, 2008). pH was measured following Standard Methods (Rice et al., 2012). For biomass quantification, the protein concentration of the biofilm on the MEC anode and carbon felt of the fermentative culture, as well as planktonic biomass were measured as previously described (Zeng et al., 2016a).

Phenolic metabolites were identified using a LC/MS-MS unit (Agilent 1260 Infinity LC system, 6410 Triple Quad MSD) equipped with a Kinetex biphenyl column (3 × 150 mm, 5 μm; Phenomenex, Torrance, CA), and a GC/MS (Agilent 7890) with a Zebtron ZB-5HT column (Phenomenex, Torrance, CA), following the procedures described in detail in Text S2. After identification, routine quantification of the metabolites was performed in duplicate using the above-described HPLC-UV method.

Cyclic voltammetry (CV) was conducted with the MEC bioanode in 24 h from the start of each batch run with SA, VA and HBA. As abiotic controls, CV was also conducted with an un-inoculated anode electrode in the presence of each of the three phenolic compounds. The potential was scanned from −0.7 to +0.3 V at a rate of 5 mV/s, with the anode as the working electrode, the cathode as the counter electrode, and the Ag/AgCl electrode (0.199 V SHE) as the reference electrode.

2.6. Calculations

Current density was calculated as the current normalized to the surface area of the cation exchange membrane, assuming the

membrane surface area was limiting, due to the narrow channel of the H-type MEC (Logan, 2012). The anode efficiency is the ratio of electron equivalents recovered as electrical current to those of substrate added. Thus, the anode efficiency is the product of chemical oxygen demand (COD) removal and Coulombic efficiency. The cathode efficiency is the ratio of electron equivalents of cathodic H_2 measured to total electrons represented by the current.

3. Results and discussion

3.1. MEC bioanode fed with SA, VA or HBA

Complete removal of the three parent compounds, SA, VA and HBA, was observed in 6 days in each respective batch run (Fig. 1A). The disappearance of SA, VA and HBA was not due to adsorption to the carbon-felt electrode or diffusion to the cathode compartment, as confirmed by our previous study on a mixture of these compounds with the same MEC materials (Zeng et al., 2015). The same study also demonstrated that under abiotic conditions, electrochemical reactions accounted for 19–22% of the transformation of SA, VA and HBA, but resulted in negligible current (Zeng et al., 2015). In the present study, the SA batch run produced a peak current density at 0.35 mA/cm^2 in 2 days (Fig. 1B). However, the peak current during the VA batch run was 0.09 mA/cm^2 , substantially lower than that of the SA batch run. Moreover, the HBA-fed bioanode produced extremely low current density ($<0.03 \text{ mA/cm}^2$), close to background levels (usually at $0.008\text{--}0.02 \text{ mA/cm}^2$ with the anolyte and catholyte in the absence of any organic substrate). Consistent with the observed current, the H_2 produced during the SA batch run ($39 \pm 0.1 \text{ mL}$; 20°C and 1 atm) was more than 7-fold higher than that produced from VA ($5 \pm 0.1 \text{ mL}$); cathodic H_2 was not detected in the HBA batch run (Fig. 1C). The three consecutive batch runs were repeated after the HBA batch run; reproducible current and H_2 production were observed with all three compounds (Fig. S1). Consistent with the current and H_2 production, cyclic voltammograms of the bioanode showed the highest overall response of current to the electrode potential change, as well as the most significant oxidation peak at around -0.2 V (vs. Ag/AgCl) in the batch run conducted with SA, whereas the current density in the VA and HBA batch runs was close to a non-fed bioanode (i.e., no substrate added in the anolyte) (Fig. S2). The oxidation peak could be attributed to redox species involved in extracellular electron transfer (e.g., outer-membrane bound proteins). Thus, the SA-fed bioanode batch run showed the highest exoelectrogenic activity, compared to that of VA and HBA. An un-inoculated anode, used as an abiotic control, produced negligible current at all potential values applied in the cyclic voltammetry for all three phenolic compounds (Fig. S2). Thus, bioactivity dominated over abiotic reactions, resulting in the removal of the parent phenolic compounds and/or the production of current. The anode pH decreased slightly from 7.0 to 6.8 during the SA batch run, and remained constant at 7.0 for the VA and HBA runs. The cathode pH remained at 7.0 for all runs conducted with the three compounds. With the voltage between the anode and the cathode controlled by the potentiostat (0.6 V), both anode and cathode potentials changed during the batch runs, ranging from -0.4 to -0.1 V for the anode and from -1.0 to -0.7 V (vs. Ag/AgCl) for the cathode. Although SA, VA and HBA may inhibit bioanode activities, the initial concentrations of the three parent compounds used in this study were below their no-observed-effect-concentration (0.8 g/L), as previously determined for the same MEC system (Zeng et al., 2016b). Thus, inhibition was not an issue or the cause of the difference in the observed exoelectrogenic activity among runs conducted with each of the three phenolic compounds.

Because the electron equivalence of the three phenolic

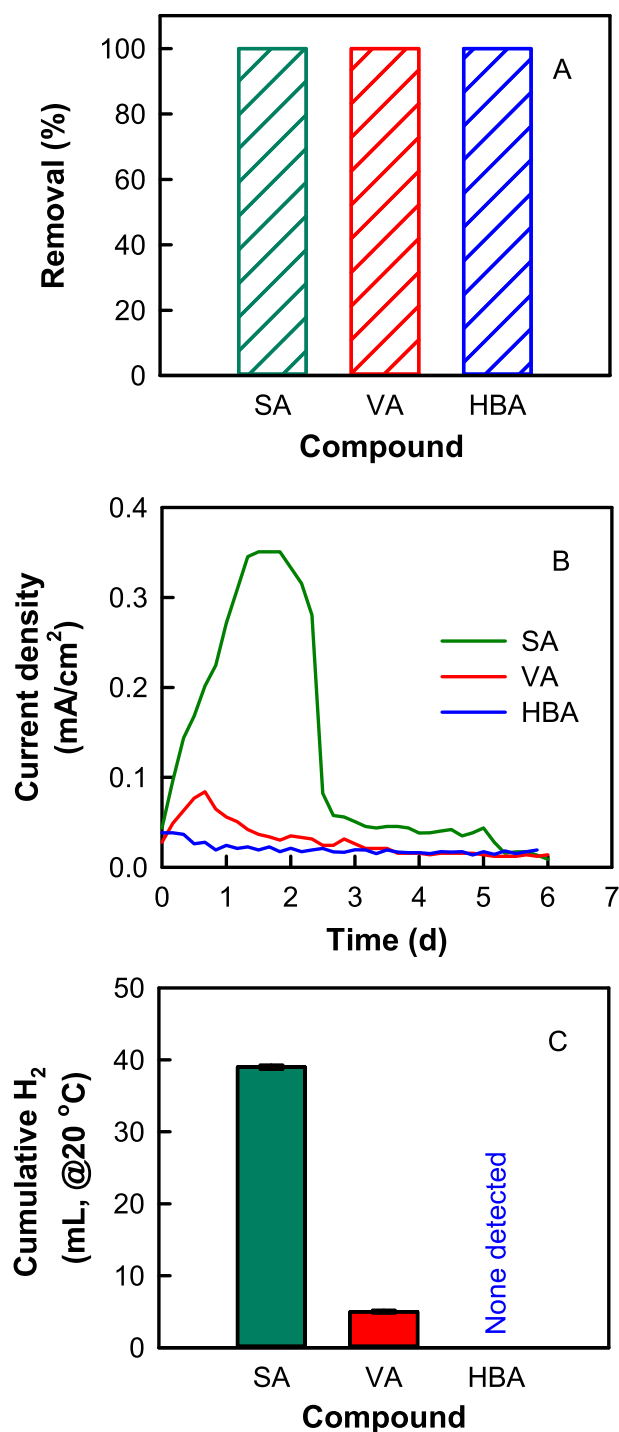


Fig. 1. —Removal of phenolic parent compounds (A), current density (B) and cathodic H_2 (C) during MEC bioanode batch runs conducted with syringic acid (SA), vanillic acid (VA) and 4-hydroxybenzoic acid (HBA). Error bars represent standard deviations, $n = 2$.

compounds is different (Table 1) whereas an equal molar concentration (1 mM) of each compound was used in the respective batch run, the total input of electron equivalents from each substrate was slightly different ($\text{SA} > \text{VA} > \text{HBA}$). Based on the electron balance performed for each batch run (Table S3), the anode efficiency was calculated as 50, 12 and 9% in the SA, VA and HBA batch runs, respectively. The cathode efficiency in the SA and VA batch runs was calculated as 81 and 76%, respectively. Cathode efficiency could

not be calculated for the HBA batch run because of the lack of H_2 production. The fact that the cathode efficiency was comparable in the SA and VA batch runs indicates that the observed difference in H_2 production is mainly attributed to the bioanode activity. Therefore, the biotransformation of SA supported bioanode exoelectrogenic activity to a much higher degree than VA and HBA, although the three phenolic compounds are structurally similar. The results of the present study provide insight into the relative contribution of individual phenolic compounds to exoelectrogenesis, which was not addressed in previous studies using mixtures of phenolic compounds as bioanode substrates (Marone et al., 2016; Zeng et al., 2015).

3.2. Biotransformation of SA, VA and HBA

3.2.1. MEC bioanode

During the SA biotransformation in the bioanode, several compounds were identified as metabolites (Fig. 2A). The first detected metabolite was 3,4-dihydroxy-5-methoxybenzoic acid (DHMBA), whose chemical structure suggests that one methyl group ($-CH_3$) was removed in the first step of SA biotransformation. The DHMBA concentration increased to 0.4 mM within 12 h and then gradually decreased to an undetectable level in the next 2 days. Following the disappearance of DHMBA, gallic acid (GA) and pyrogallol were detected as two metabolites. The chemical structures of GA and pyrogallol indicate that a second demethylation step occurred,

removing the $-CH_3$ group from DHMBA, resulting in GA, followed by a decarboxylation step eliminating the $-COOH$ group from GA, leading to the production of pyrogallol. Both GA and pyrogallol were transient metabolites detected at a maximum concentration of 0.15 and 0.07 mM, respectively, in 1.5 days (Fig. 2A). Pyrogallol was the last aromatic metabolite detected, and could potentially be the last product before the aromatic ring cleavage. Other assumed metabolites, such as catechol, phenol and benzoic acid listed in Table S1, were not detected during the biotransformation of SA.

The above-mentioned SA metabolites were also reported by Kaiser and Hanselmann (1982), who studied SA biotransformation in a fermentative/methanogenic culture enriched from a freshwater lake sediment. In addition, the same study reported further fermentation of pyrogallol to acetate at a stoichiometric amount (3 mol) under methanogenesis-inhibited conditions, demonstrating that the aromatic ring of pyrogallol was cleaved by fermentative bacteria, independently from a syntrophic association with methanogens. In the present study, acetate was not detected during the SA batch run in the bioanode as a result of a rapid acetate consumption by the active exoelectrogens, given that acetate is a major substrate used by exoelectrogens (Wang and Ren, 2013). The high exoelectrogenic activity in the SA batch run, in turn, indicates that a significant quantity of acetate was produced. As reported in our previous studies, acetate was detected only with an open circuit (i.e., in the absence of exoelectrogenesis) or when exoelectrogenesis was inhibited (Zeng et al., 2015, 2016a). Direct evidence of

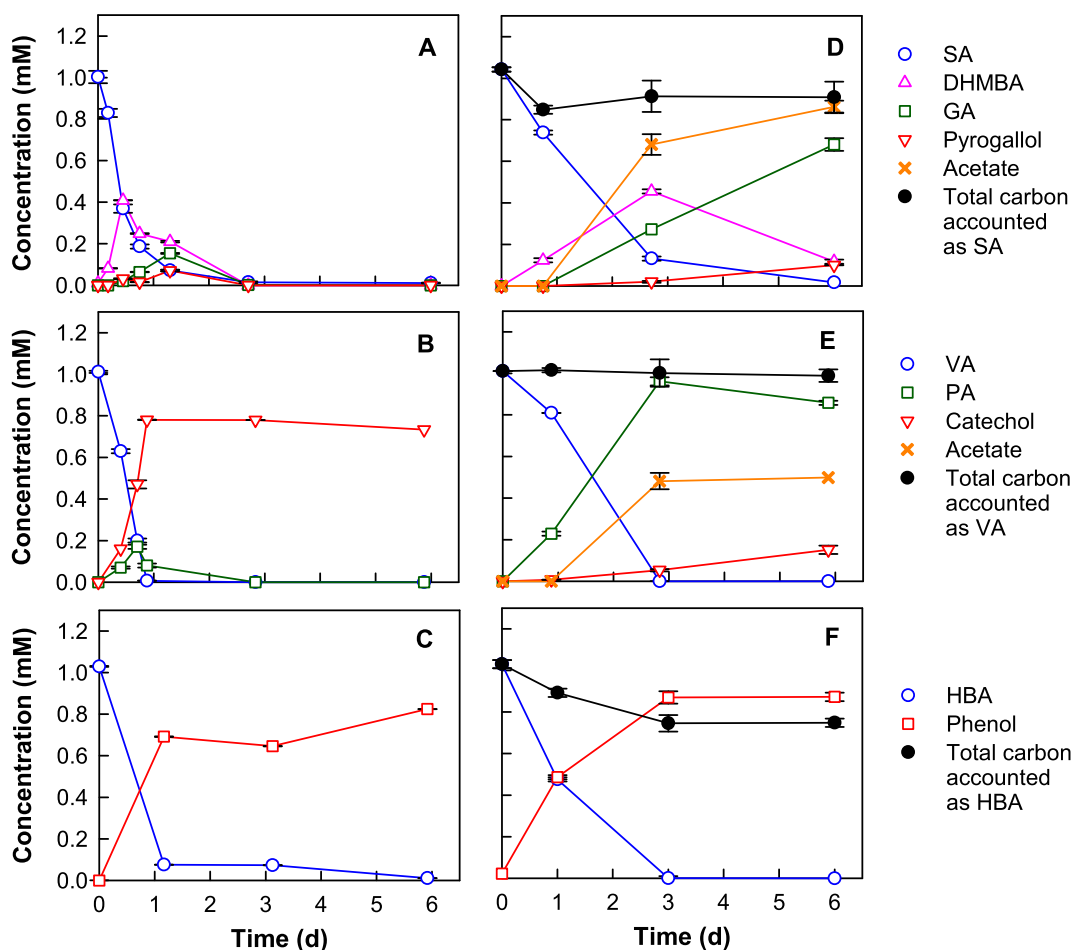
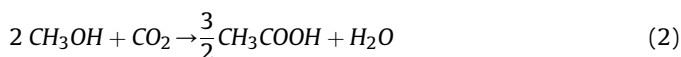
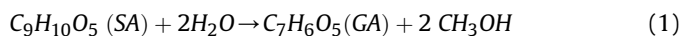


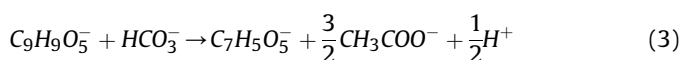
Fig. 2. Biotransformation products of SA, VA and HBA in MEC bioanode (A, B, C) and fermentative culture (D, E, F) batch runs. Error bars represent standard deviations, $n = 2$. Abbreviations: SA, syringic acid; DHMBA, 3,4-dihydroxy-5-methoxybenzoic acid; GA, gallic acid; VA, vanillic acid; PA, protocatechuic acid; HBA, 4-hydroxybenzoic acid.

acetate production from SA is provided by the fermentative batch run, discussed in Section 3.2.2, below.

Acetate can be produced not only from aromatic ring cleavage, but also from the demethylation of methoxy groups. Bache and Pfennig (1981) reported that methoxy carbons on aromatic compounds were first removed from the aromatic ring, resulting in methanol (eq (1)), which was subsequently converted to acetate in the presence of bicarbonate (eq (2)).



The overall reaction at neutral pH can be written as follows:



The conversion of methoxy carbon to acetate was confirmed in *Acetobacterium woodii*, an acetogenic, fermentative bacterium, growing on methoxy groups of various aromatic compounds (including SA and VA) without cleaving the aromatic rings. For every 1 mol methoxy group removed, 0.75 mol of acetate was produced (Bache and Pfennig, 1981). As discussed in Section 3.3, below, *Acetobacterium* was present in the MEC bioanode used in the present study. In addition, bicarbonate could be produced by the decarboxylation of GA to pyrogallol, as well as from the oxidation of acetate during exoelectrogenesis. Thus, it is plausible that two demethylation steps of SA could have resulted in 1.5 mM acetate. Based on the electron equivalence of acetate (8 e[−]/mol/mol) and the current produced during the SA batch run, the minimum amount of acetate used for exoelectrogenesis was back calculated as 2.5 mM, assuming 100% Coulombic efficiency. Thus, the acetate produced from the methoxy groups of SA (1.5 mM maximum) was not enough to support the observed exoelectrogenesis. Instead, aromatic ring cleavage must have contributed to the calculated acetate production.

VA biotransformation resulted in two aromatic metabolites, protocatechuic acid (PA) and catechol (Fig. 2B). Similar to SA, demethylation occurred, removing the methoxy carbon from VA, resulting in PA production. Subsequently, decarboxylation of PA led to the production of catechol. PA was detected at low levels (<0.2 mM) with a transient appearance in the first 3 days. In contrast, catechol was formed in 1 day, reaching a high concentration (0.8 mM) and was persistent throughout the 6-day batch run. Because VA and catechol are both mono-aromatic compounds, 1 mM VA is expected to produce 1 mM catechol at most. Thus, the detected catechol (0.8 mM) accounted for 80% of the VA added, making catechol a major dead-end product. The conversion of VA to PA and then to catechol has been reported in a fermentative/methanogenic culture enriched from a freshwater sediment (Kaiser and Hanselmann, 1982). The same study reported that catechol was persistent throughout the 2-week incubation, and suggested that only aromatic compounds with three hydroxyl or methoxy substituents were degraded via ring cleavage. These previous findings are in agreement with the observations during SA and VA biotransformation in the present study.

As discussed above, methoxy carbons on methoxylated aromatic compounds can be converted to acetate with a stoichiometric coefficient of 0.75 mol-acetate/mol-methoxy group. Acetate produced by the demethylation of VA, in spite of an intact aromatic ring, may explain the small current peak observed on day 1 during the VA biotransformation (Fig. 1B). The total current observed during the VA batch run requires at least 0.53 mM of acetate, back calculated based on the above-mentioned electron equivalence of acetate.

This minimum acetate demand is close to the concentration that can be produced from the methoxy group of VA (0.75 mM). In comparison, SA has twice the amount of methoxy carbons (Table 1), but the current resulting from the biotransformation of SA was 7-fold higher than that of VA. Thus, the number of methoxy groups in SA and VA cannot fully explain the difference in the observed exoelectrogenic activity.

Catechol is a dihydroxylated metabolite produced from VA, analogous to pyrogallol, a trihydroxylated benzene derived from SA. However, the persistence of catechol is in contrast to the transient fate of pyrogallol. Thus, the biotransformation pathway of SA and VA becomes significantly different after the initial, common steps of demethylation and decarboxylation. The relatively low extent of VA fermentative biotransformation is consistent with the observed low exoelectrogenic activity, while the higher extent of SA biotransformation resulted in a higher exoelectrogenic activity. Therefore, the difference in the exoelectrogenic activity of the SA and VA batch runs is not only related to the number of methoxy groups of the substrate, but more importantly to the extent of the fermentative biotransformation, i.e., aromatic ring cleavage or not.

HBA biotransformation resulted in phenol as the only detected metabolite (Fig. 2C), resulting from the decarboxylation of HBA. Phenol was detected at high levels (0.7–0.8 mM) and was persistent throughout the 6-day batch run. Thus, as in the above-discussed VA biotransformation, HBA was biotransformed mainly to a dead-end product representing 80% of the HBA added. Moreover, HBA does not contain any methoxy substituent which could lead to the production of acetate. The combination of the low extent of biotransformation and the lack of a methoxy group led to extremely low exoelectrogenic activity in the HBA-fed bioanode (Fig. 1). Benzoic acid, an assumed metabolite, was not consistently detected in all samples and its concentration was negligible (<0.02 mM). Therefore, benzoic acid is not considered an important metabolite of HBA under the experimental conditions of the present study. The biotransformation of HBA to phenol has been reported in an enriched fermentative/methanogenic culture (Tschuch and Schink, 1986), anoxic aquifer samples (Kuhn et al., 1989), and a pure culture of *Clostridium* strain JW/Z-1 (Zhang and Wiegel, 1990).

Transient pyrogallol levels, as well as persistent catechol and phenol, were observed in repeated consecutive batch runs conducted with SA, VA or HBA (data not shown), confirming the reproducibility of the above-discussed results of the first round batch runs. The chemical structures of the above-mentioned metabolites were confirmed by their mass spectra obtained from LC/MS-MS (Fig. S3). All identified compounds had fragmentation patterns identical to those of the analytical standards. Phenolic acids, such as DHMBA, GA and PA, mainly yielded fragments at m/z of [M-1] and [M-45], representing the loss of a H⁺ and a -COOH, respectively. In the mass spectra of pyrogallol and catechol, large fragment peaks appeared at m/z of [M-1] and [M-2], along with other small peaks. The abundant [M-1] and [M-2] peaks were attributed to the elimination of H⁺ from the -OH groups. The phenol mass spectrum in GC/MS showed a strong molecular peak (m/z = 94) and a fragment peak at m/z of [M-28], resulting from the loss of a carbon monoxide (Fig. S4).

3.2.2. Fermentative culture

In order to further delineate the role of fermentative biotransformation in the MEC bioanode, the biotransformation of SA, VA and HBA was also evaluated in consecutive batch runs conducted using the fermentative culture. This culture, which was inoculated with the microbial community from the MEC bioanode (see Section 2.2, above), represents an open circuit control under non-exoelectrogenic conditions.

SA biotransformation resulted in the production of DHMBA, GA,

pyrogallol and acetate (Fig. 2D). The detected metabolites represented a carbon recovery of 85–90%, while a small fraction of carbon could have been used for biomass synthesis. The detected aromatic metabolites were identical to those found in the MEC bioanode batch runs, except for acetate, which was not detected in the bioanode but accumulated to a high level (0.86 mM) in the fermentative culture. Because there was no acetate-consuming process in the fermentative culture, such as exoelectrogenesis or methanogenesis, acetate accumulated as an end product. The observed acetate level (0.86 mM) was lower than the calculated acetate demand (2.5 mM), corresponding to the observed exoelectrogenic activity in the SA bioanode batch run. The difference in acetate levels is attributed to the different rate of biotransformation in the bioanode and the fermentative culture, resulting in a different extent of biotransformation. The biomass concentration in the fermentative culture was 7-fold lower than that in the bioanode (47.2 vs. 352 mg/L as protein; Sections 2.2 and 2.3, above). Consequently, the biotransformation rate was lower in the fermentative batch run (Fig. 2A vs. 2D). Thus, for the same incubation time of 6 days, a lower extent of biotransformation was achieved in the runs conducted with the fermentative culture, resulting in a relatively lower acetate concentration at the end of the batch run. The difference in the biomass concentration between the MEC bioanode and the fermentative culture is attributed to the length of time each system had been maintained (2 years vs. 4 months, respectively; see Sections 2.2 and 2.3). Exoelectrogens, which consume fermentation products, could be beneficial to the growth of fermenters in the MEC bioanode. However, whether or not and to what extent syntrophic relationships in the bioanode benefited the growth of fermenters, is not clear.

VA biotransformation in the fermentative culture resulted in the production of PA and catechol (Fig. 2E), the same metabolites detected in the VA bioanode batch run. As discussed above, due to the lower biomass concentration in the fermentative culture than in the bioanode, the concentrations of the observed metabolites were lower than those in the MEC bioanode run. For instance, catechol did not reach a level as high as that found in the bioanode for the same incubation time (6 d). Nevertheless, a nearly 100% carbon balance was achieved. Acetate was produced and remained at 0.5 mM after VA was completely transformed. As discussed above, the methoxy carbon on VA can be converted to acetate at a stoichiometric amount of 0.75 mM/mM VA, which is slightly higher than the measured acetate concentration.

HBA biotransformation in the fermentative culture resulted in the production of phenol as the only detected metabolite, representing 75% of the HBA added. Acetate was not detected throughout the 6-d incubation period (Fig. 2F). The persistence and dominance of phenol during the HBA biotransformation is consistent with the observed low exoelectrogenic activity of the MEC bioanode batch run. The lack of acetate production in this fermentation run also agrees with the observed negligible exoelectrogenesis during the MEC bioanode run. Carbon balance analysis showed that 25% of the initially added carbon was not accounted for by the detected metabolite (i.e., phenol). It is noteworthy that 1 mM HBA converted to phenol by decarboxylation can result in 1 mM bicarbonate, representing 12.5% of the total added carbon. The remaining 12.5% of unaccounted carbon might be attributed to un-identified metabolites formed in minor biotransformation pathways and/or microbial growth.

Considering that the main metabolic processes in a bioanode are fermentation followed by exoelectrogenesis, acetate production through fermentation of the phenolic substrates is critical to the exoelectrogenic activity. In the fermentative batch runs, SA produced the highest concentration of acetate (0.86 mM) followed by VA (0.5 mM), but HBA did not result in acetate production. The

amount of acetate produced from SA, VA and HBA is consistent with the relative exoelectrogenic activity in the MEC bioanode batch runs conducted with these compounds. Nevertheless, it is noteworthy that the measured acetate concentration does not represent the ultimate acetate-producing capacity of these compounds because of the limited duration of the fermentative batch runs, which in turn resulted in a limited extent of biotransformation. Qualitatively, the fermentative transformation of the three phenolic compounds resulted in the production of aromatic metabolites identical to those detected in the MEC bioanode batch runs. Therefore, the fermentative transformation of the three phenolic compounds in the MEC bioanode took place independently of exoelectrogenesis.

3.2.3. Biotransformation pathways

Based on the chemical structures and the sequence of detected metabolites, biotransformation pathways of SA, VA and HBA in the MEC bioanode are proposed (Fig. 3). Demethylation and decarboxylation were common reactions employed to remove the $-\text{CH}_3$ from $-\text{O}-\text{CH}_3$ groups and the $-\text{COOH}$ substituents from aromatic rings, resulting in hydroxylated analogs of SA, VA and HBA (i.e., pyrogallol, catechol and phenol, respectively). As demonstrated in fermentative batch runs (Section 3.2.2, above), these reactions could occur through fermentation, independent of exoelectrogenesis. *O*-demethylase and decarboxylase, catalyzing the demethylation and decarboxylation reactions, respectively, have been found and characterized in *Acetobacterium* spp. (Kaufmann et al., 1998), *Pelobacter acidigallici* (Brune and Schink, 1992), and *Clostridium hydroxybenzoicum* (He and Wiegand, 1995). As discussed in Section 3.3, below, *Acetobacterium*, *Pelobacter*, and *Clostridium* spp. were detected in the MEC bioanode and the fermentative culture biofilm microbial communities.

After the common demethylation and decarboxylation steps, subsequent reactions in the biotransformation pathways after the production of pyrogallol, catechol and phenol differed. As discussed in Sections 3.2.1 and 3.2.2, above, the aromatic ring of pyrogallol was cleaved, resulting in the production of acetate under both bioanode and fermentative conditions. However, catechol and phenol remained intact as major and persistent metabolites. Consistent with the results reported here, during the enrichment of the bioanode and the fermentative culture, when SA, VA and HBA were used as substrates in a mixture with furanic compounds, the removal of parent phenolic compounds, as well as the accumulation of catechol and phenol were observed. Although SA has a higher extent of biotransformation than VA and HBA, as shown in the present study, preferential substrate utilization was not observed when these compounds were added to the MEC bioanode as a mixture (Zeng et al., 2015).

Aromatic ring cleavage under anoxic conditions is possible by reductive reactions, which requires the formation of central intermediates possessing strong electron-withdrawing substituents, thus facilitating electron transfer to the ring (Fuchs et al., 2011). One group of such central intermediates is aromatic compounds with two or more hydroxyl groups in the *meta* position relative to each other, such as resorcinol (1,3-dihydroxybenzene) and phloroglucinol (1,3,5-trihydroxybenzene), which have mesomeric non-aromatic structures and weakened aromatic stability (Schink et al., 2000). Another group of central intermediates is CoA-thioester substituted aromatic compounds, such as benzoyl-CoA. The aromatic ring of such central intermediates can be cleaved by reduction and/or hydrolysis (Schink et al., 2000). Pyrogallol (1,2,3-trihydroxybenzene) detected in the present study could not be hydrolyzed or directly reduced (Schink et al., 2000). However, through a transhydroxylation reaction, pyrogallol can be isomerized to phloroglucinol (Brune and Schink, 1990), which can

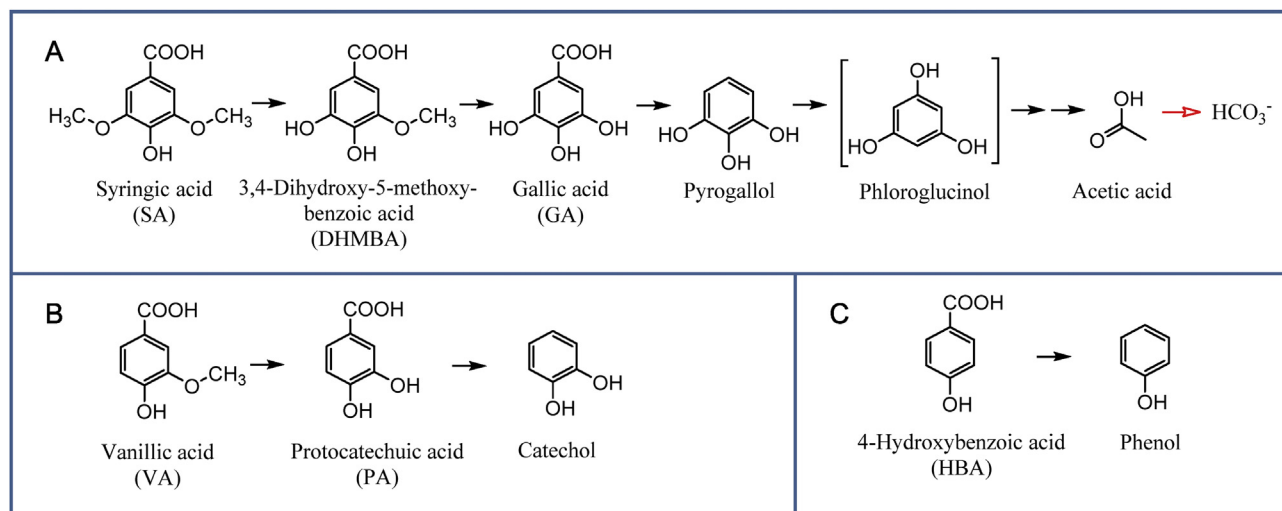


Fig. 3. Proposed biotransformation pathways of SA (A), VA (B) and HBA (C) under MEC bioanode conditions based on identified metabolites. Solid arrows denote fermentative steps; hollow arrow denotes exoelectrogenic step. Phloroglucinol in brackets is a hypothetical metabolite.

then be easily reduced by a conventional NADPH-dependent reductase and hydrolyzed to yield 3 mol of acetate (Fig. S5) (Schink et al., 2000). The reaction of pyrogallol-to-phloroglucinol isomerization ($\Delta G^\circ = -15.5$ kJ/mol) is a well-established pyrogallol degradation mechanism in fermentative bacteria, such as *Eubacterium oxidoreducens* and *Pelobacter acidigallici* (Brune and Schink, 1990, 1992; Haddock and Ferry, 1989). In the present study, the detection of both *Eubacterium* and *Pelobacter* species in the MEC bioanode microbial community (Section 3.3, below) and acetate as a fermentation product, support the phloroglucinol pathway in the pyrogallol degradation. Although phloroglucinol was not detected, which might be due to a fast consumption rate, it is included in the SA biotransformation pathway as a hypothetical intermediate (Fig. 3A).

Catechol and phenol cannot undergo transhydroxylation reactions to form phloroglucinol or resorcinol, as is the case of pyrogallol (Brune and Schink, 1990). Thus, an alternative route for anaerobic ring cleavage (i.e., benzoyl-CoA pathway) is required for catechol and phenol degradation. The benzoyl-CoA pathway has been demonstrated in sulfate- and nitrate-reducing bacteria (*Desulfobacterium*, *Thauera aromatica* and *Azoarcus* spp.) for catechol and phenol degradation. In this pathway, a carboxylation step is required to convert catechol and phenol to protocatechuic acid (PA) and 4-hydroxybenzoic acid (HBA), respectively, prior to the addition of CoA thioesters (Gorny and Schink, 1994; Tschech and Fuchs, 1989; van Schie and Young, 1998). However, the biotransformation observed in the present study occurred in the opposite direction (i.e., PA to catechol and HBA to phenol; Fig. 3). Thus, the benzoyl-CoA pathway was not used or was of minor importance in the present study. Otherwise, PA and HBA would have been converted to protocatechuyl-CoA and 4-hydroxybenzoyl-CoA, instead of catechol and phenol. The reason why VA (or PA) and HBA were not converted to benzoyl-CoA is unclear, but plausible explanations are discussed below. The benzoyl-CoA pathway is energy intensive. Benzoyl-CoA degradation yields 3 ATP equivalents, but the formation of benzoyl-CoA consumes 2 ATP equivalents (Fuchs et al., 2011). Thus, it is particularly difficult for fermentative bacteria, which do not have a respiratory chain as do nitrate and sulfate reducers, to generate the ATP equivalents needed for the benzoyl-CoA pathway, unless an ATP-independent ring reduction mechanism is used (Fuchs et al., 2011). Furthermore, the carboxylation of catechol to PA

or phenol to HBA requires additional ATP, making the overall energy balance extremely demanding (Schink et al., 2000; Fuchs et al., 2011). In comparison, decarboxylation reactions (i.e., PA to catechol and HBA to phenol) can generate ATP by creating a proton gradient across the cell membrane (Schie and Young, 2000). The free energy change in the reaction of HBA decarboxylation to phenol was estimated as -19 to -21 kJ/mol (Brune and Schink, 1992). Thus, the decarboxylation reaction is more physiologically advantageous than the benzoyl-CoA pathway, which may partially explain the persistence of catechol and phenol in the present study. Catechol and phenol are highly prone to aerobic biodegradation (Fuchs et al., 2011). Thus, in MFCs with air cathodes, where oxygen can diffuse into the bioanode (Zhang et al., 2015), catechol and phenol degradation can be highly favored. Oxygen diffusion may have partially accounted for phenol removal reported in previous MFC studies (Song et al., 2014; Luo et al., 2009; Friman et al., 2013). In addition, if the bioanode feed contains significant levels of alternative electron acceptors (i.e., nitrate, iron (III), or sulfate), the degradation of catechol and phenol may occur via anaerobic respiration using the benzoyl-CoA pathway as mentioned above. However, the presence of such alternative electron acceptors will divert electrons from exoelectrogenesis, thus lowering the MEC Coulombic efficiency.

Table S2 lists the standard Gibbs free energy change (ΔG° , pH 7 and 298 K) of potential fermentation reactions of SA, VA, HBA, pyrogallol, catechol and phenol. Fermentation products of each compound were hypothesized based on the stoichiometry of demethylation (0.75 mol-acetate/mol-methoxy group), decarboxylation (1 mol HCO_3^- /mol-carboxyl group), and aromatic ring cleavage (3 mol-acetate/mol-aromatic ring). H_2 and H_2O were added accordingly to balance the reactions. The calculated ΔG° values are negative for all compounds, except for phenol (+8.46 kJ/mol), indicating that the hypothetical fermentation reactions are favorable for SA, VA, HBA, catechol and pyrogallol, without the need of syntrophic H_2 -utilizing partners. However, experimental results showed that catechol was persistent, despite the negative ΔG° value for catechol fermentation. Thus, thermodynamics cannot fully explain the persistence of catechol and phenol observed in the present study. For the endergonic reaction (i.e., phenol fermentation) to take place, a syntrophic partner consuming the fermentation products is required to achieve a negative ΔG value. Under the MEC bioanode conditions, exoelectrogens can act as syntrophic partners utilizing acetate and H_2 produced from fermentation, as

previously demonstrated in a glucose-fed bioanode (Freguia et al., 2008). Homoacetogens, represented by *Acetobacterium*, were also important in the syntrophy as H_2 scavengers (Parameswaran et al., 2010). In fact, acetate or H_2 was not detected in any of the bioanode batch runs in the present study. Therefore, the persistence of catechol and phenol in the MEC bioanode was not related to the lack of syntrophic interactions.

To assess whether the low extent of VA and HBA biotransformation was due to the lack of requisite microbial species, biotransformation assays of SA, VA and HBA were conducted with diverse microbial communities in environmental samples obtained from a pulp and paper mill lagoon sediment (Dykstra et al., 2015) and a contaminated estuarine sediment (Gess and Pavlostathis, 1997). In both assays, SA, VA and HBA were converted in 30 days after a lag phase of 7–20 days, resulting in catechol and phenol as the predominant metabolites from VA and HBA, respectively. However, after 763 days of incubation, catechol and phenol were still persistent at the same level in the pulp and paper sediment assay, whereas they were completely transformed in the contaminated sediment assay. Literature-reported fate of catechol and phenol under fermentative/methanogenic conditions varies from study to study, as discussed below. Kaiser and Hanselmann (1982) and Tschuch and Schink (1986) observed persistent catechol produced from VA. In a review by Schink et al. (2000), catechol was regarded as the most slowly degraded divalent phenol under anoxic conditions. Tschuch and Schink (1986) reported that phenol, produced from HBA, was slowly degraded in several weeks, whereas Kuhn et al. (1989) observed a fast degradation of phenol in 4 days. An earlier study reported that all SA, VA, HBA, catechol and phenol were degraded within 34 days, with more than 60% of the carbon converted to CH_4 and CO_2 (Healy and Young, 1979). In contrast to the aforementioned studies, all conducted with pure chemicals, a recent MEC study, which used a complex aqueous organic mixture generated during pyrolysis of switchgrass, observed removal of catechol and phenol (Lewis et al., 2015). The presence of readily biodegradable components in the switchgrass-derived stream (e.g., acetate, sugars), may have facilitated the degradation of catechol and phenol. Therefore, the fate of catechol and phenol in the above-mentioned studies varied, depending on microbial communities, metabolic conditions and rates.

3.3. Microbial communities

The composition of the bioanode microbial community characterized after 6 months of enrichment (in MFC), as well as after 7 and 13 months (in MEC) is presented in Table S4. The results of the latter two microbial community analyses were previously discussed in detail (Zeng et al., 2015, 2016a). Here, we present an overview of the bioanode biofilm microbial community established during the long-term bioanode development, as compared to the microbial community of the fermentative culture. The three samples of the bioanode microbial community (i.e., MFC-6 month, MEC-7 month, and MEC-13 month) consisted of the same major phyla at comparable relative abundances: *Proteobacteria* (68–85%), *Bacteroidetes* (2–17%), and *Firmicutes* (9–12%) (Table S4). The *Proteobacteria* phylum was dominated by *Geobacter* or *Desulfovibrio* genera (>30%), which are considered as putative exoelectrogens (Logan, 2009; Kang et al., 2014). The MEC-7 month sample was less abundant in *Geobacter* spp. and more abundant in *Desulfovibrio* spp., compared to the MFC-6 month sample, possibly as a result of community transfer from the MFC to the MEC bioanode. Nevertheless, after several months of MEC operation, the abundance of *Geobacter* and *Desulfovibrio* spp. observed in the MEC-13 month sample was similar to that in the MFC-6 month sample. *Pelobacter* genus, which includes species degrading pyrogallol (Brune and

Schink, 1992), was detected in *Proteobacteria* (0.2–1.7%). In the *Firmicutes* phylum, genera of *Eubacterium*, *Acetobacterium*, *Anaerovorax*, and *Clostridium* were present in the three bioanode samples at an abundance within the same order of magnitude. As discussed above, *Eubacterium*, *Acetobacterium*, *Clostridium*, and *Pelobacter* spp. have been reported to anaerobically transform phenolic compounds (Bache and Pfennig, 1981; Zhang and Wiegand, 1990; Brune and Schink, 1990, 1992; Haddock and Ferry, 1989; He and Wiegand, 1995). It is noteworthy that the same microbial phylotypes were found in the bioanode at different stages of the present study, although at a variable abundance at the genus level. Thus, the long-term MEC operation with the same substrate mixture as bioanode feed resulted in a well-established bioanode microbial community. Although 6-d batch runs using individual phenolic compounds were conducted in the present study, such short-term experiments should not have significantly altered the bioanode biofilm microbial community structure.

The microbial community of the fermentative culture biofilm, characterized 6 months after the startup, was dominated by *Proteobacteria* (60%), *Bacteroidetes* (28%), and *Firmicutes* (12%) (Table S4). Abundant species (i.e., >1% of total sequences) within the *Proteobacteria* phylum belonged to the genera of *Azoarcus* (33%), *Pseudomonas* (24%), and *Magnetospirillum* (2%). In the *Firmicutes* phylum, abundant phylotypes were distributed in genera of *Acetobacterium* (8%), *Anaerovorax* (2%), and *Clostridium* (1%).

The similarity and dissimilarity between the microbial communities of the bioanode and the fermentative culture biofilms are discussed below. First, the two microbial communities are highly similar at the phylum level, and all genera detected in the fermentative culture were present in the bioanode (Table S4). Second, several abundant genera in the bioanode were found at levels order(s) of magnitude lower in the fermentative culture, including *Geobacter*, *Desulfovibrio*, *Eubacterium*, and *Pleomorphomonas*. As mentioned above, *Geobacter* and *Desulfovibrio* are putative exoelectrogens, which were expected to be less predominant in the non-exoelectrogenic, fermentative culture. It is not clear why *Eubacterium* and *Pleomorphomonas* were also considerably less abundant in the fermentative culture biofilm. In contrast, the relative abundance of *Pseudomonas*, *Proteiniphilum*, and *Acetobacterium* spp. was order(s) of magnitude higher in the fermentative culture biofilm than in the bioanode biofilm. The members of *Pseudomonas* genus can use many different organic compounds as carbon and energy sources, both aerobically and anaerobically (Madigan et al., 2009). Such metabolic diversity makes it difficult to identify the reason why *Pseudomonas* spp. were enriched in the fermentative culture. *Proteiniphilum* spp. are proteolytic, obligate anaerobic bacteria (Chen and Dong, 2005), which may have grown on dead cell material in the fermentative culture. *Acetobacterium* spp., which is an important phenolic degrader, as mentioned above (Bache and Pfennig, 1981; Kaufmann et al., 1998), could grow favorably in the fermentative culture. In summary, consistent with the fact that the fermentative culture was inoculated with the MEC bioanode microbial community, common phylotypes were shared between the two microbial communities. However, due to the difference in metabolic conditions (exoelectrogenic vs. non-exoelectrogenic), putative exoelectrogens were nearly absent in the fermentative culture, and differences were observed in relative abundance at the genus level of other species.

4. Conclusions

The great difference in the extent of fermentative biotransformation of SA, VA and HBA shown in the present study is rooted in the number and position of their $-OH$ and $-O-CH_3$ substituents. The syringyl arrangement of the $-OH$ and $-O-CH_3$ groups enables

the transformation of SA to pyrogallol, whose aromatic ring can be easily cleaved using the well-established phloroglucinol pathway even under strict fermentative conditions. In contrast, the guaiacyl and *p*-hydroxyphenyl position of –OH and –O–CH₃ in VA and HBA does not support the formation of a trihydroxylated benzene as a central intermediate that can then enter the phloroglucinol pathway. Instead, VA and HBA are decarboxylated to dead-end products such as catechol and phenol, respectively. The higher extent of fermentative transformation of SA explains the higher exoelectrogenic activity in the SA-fed bioanode batch run, compared to that of VA and HBA. These findings shed light on the fate of individual phenolic compounds in bioanodes of bio-electrochemical systems, which have been recognized as an integrative technology for waste and water management in biofuel production. To overcome metabolic limitations in MEC bioanodes, selective enrichment of fermentative bacteria, capable of metabolizing complex compounds to a high extent, should be considered. On the other hand, it is also important for future studies to discover and/or engineer exoelectrogenic species capable of directly utilizing a wider range of complex substrates.

Notice of copyright

This manuscript has been co-authored by UT-Battelle, LLC under Contract No. DE-AC05-00OR22725 with the U.S. Department of Energy. The United States Government retains and the publisher, by accepting the article for publication, acknowledges that the United States Government retains a non-exclusive, paid-up, irrevocable, world-wide license to publish or reproduce the published form of this manuscript, or allow others to do so, for United States Government purposes. The Department of Energy will provide public access to these results of federally sponsored research in accordance with the DOE Public Access Plan (<http://energy.gov/downloads/doe-public-access-plan>).

Acknowledgements

We acknowledge funding for this work from the U.S. Department of Energy, BioEnergy Technologies Office under the Carbon, Hydrogen and Separations Efficiency (CHASE) in Bio-Oil Conversion Pathways program, DE-FOA-0000812. Oak Ridge National Laboratory is managed by UT-Battelle, LLC, for the US Department of Energy under contract DE-AC05-00OR22725.

Appendix A. Supplementary data

Supplementary data related to this article can be found at <http://dx.doi.org/10.1016/j.watres.2016.11.057>.

References

- Bache, R., Pfennig, N., 1981. Selective isolation of *Acetobacterium woodii* on methoxylated aromatic acids and determination of growth yields. *Arch. Microbiol.* 130 (3), 255–261.
- Borole, A., Mielenz, J., Vishnivetskaya, T., Hamilton, C., 2009. Controlling accumulation of fermentation inhibitors in biorefinery recycle water using microbial fuel cells. *Biotechnol. Biofuel.* 2 (1), 7.
- Borole, A.P., Mielenz, J.R., 2011. Estimating hydrogen production potential in biorefineries using microbial electrolysis cell technology. *Int. J. Hydrogen Energy* 36 (22), 14787–14795.
- Borole, A.P., Hamilton, C.Y., Schell, D.J., 2013. Conversion of residual organics in corn stover-derived biorefinery stream to bioenergy via a microbial fuel cell. *Environ. Sci. Technol.* 47 (1), 642–648.
- Brune, A., Schink, B., 1990. Pyrogallol-to-phloroglucinol conversion and other hydroxyl-transfer reactions catalyzed by cell extracts of *Pelobacter acidigallici*. *J. Bacteriol.* 172 (2), 1070–1076.
- Brune, A., Schink, B., 1992. Phloroglucinol pathway in the strictly anaerobic *Pelobacter acidigallici*: fermentation of trihydroxybenzenes to acetate via triacetic acid. *Arch. Microbiol.* 157 (5), 417–424.
- Chemaxon calculator plugins, <http://www.chemaxon.com>.
- Chen, S., Dong, X., 2005. *Proteiniphilum acetatigenes* gen. nov., sp. nov., from a UASB reactor treating brewery wastewater. *Int. J. Syst. Evol. Microbiol.* 55 (6), 2257–2261.
- Dykstra, C.M., Giles, H.D., Banerjee, S., Pavlostathis, S.G., 2015. Fate and biotransformation of phytosterols during treatment of pulp and paper wastewater in a simulated aerated stabilization basin. *Water Res.* 68, 589–600.
- Freguia, S., Rabaey, K., Yuan, Z., Keller, J., 2008. Syntrophic processes drive the conversion of glucose in microbial fuel cell anodes. *Environ. Sci. Technol.* 42 (21), 7937–7943.
- Friman, H., Schechter, A., Ioffe, Y., Nitzan, Y., Cahan, R., 2013. Current production in a microbial fuel cell using a pure culture of *Cupriavidus basilensis* growing in acetate or phenol as a carbon source. *Microb. Biotechnol.* 6 (4), 425–434.
- Fuchs, G., Boll, M., Heider, J., 2011. Microbial degradation of aromatic compounds — from one strategy to four. *Nat. Rev. Microbiol.* 9 (11), 803–816.
- Gess, P., Pavlostathis, S.G., 1997. Desorption of chlorinated organic compounds from a contaminated estuarine sediment. *Environ. Toxicol. Chem.* 16 (8), 1598–1605.
- Gorny, N., Schink, B., 1994. Anaerobic degradation of catechol by *Desulfobacterium* sp. strain CAT2 proceeds via carboxylation to protocatechuate. *Appl. Environ. Microbiol.* 60 (9), 3396–3400.
- Haddock, J.D., Ferry, J.G., 1989. Purification and properties of phloroglucinol reductase from *Eubacterium oxidoreducens* G-41. *J. Biol. Chem.* 264 (8), 4423–4427.
- He, Z., Wiegel, J., 1995. Purification and characterization of an oxygen-sensitive reversible 4-hydroxybenzoate decarboxylase from *Clostridium hydroxybenzoicum*. *Eur. J. Biochem.* 229 (1), 77–82.
- Healy, J.B., Young, L.Y., 1979. Anaerobic biodegradation of eleven aromatic compounds to methane. *Appl. Environ. Microbiol.* 38 (1), 84–89.
- Hedbavna, P., Rolfe, S.A., Huang, W.E., Thornton, S.F., 2016. Biodegradation of phenolic compounds and their metabolites in contaminated groundwater using microbial fuel cells. *Bioresour. Technol.* 200, 426–434.
- Huang, D.-Y., Zhou, S.-G., Chen, Q., Zhao, B., Yuan, Y., Zhuang, L., 2011. Enhanced anaerobic degradation of organic pollutants in a soil microbial fuel cell. *Chem. Eng. J.* 172 (2–3), 647–653.
- Jones, S., Holladay, J., Valkenburg, C., Stevens, D., 2009. Production of Gasoline and Diesel from Biomass via Fast Pyrolysis, Hydrotreating and Hydrocracking: a Design Case. Pacific Northeast National Laboratory, Richland, WA. PNNL-18284.
- Kaiser, J.-P., Hanselmann, K., 1982. Fermentative metabolism of substituted monoaromatic compounds by a bacterial community from anaerobic sediments. *Arch. Microbiol.* 133 (3), 185–194.
- Kang, C.S., Eaktsang, N., Kwon, D.Y., Kim, H.S., 2014. Enhanced current production by *Desulfovibrio desulfuricans* biofilm in a mediator-less microbial fuel cell. *Bioresour. Technol.* 165, 27–30.
- Kaufmann, F., Wohlfarth, G., Diekert, G., 1998. O-demethylase from *Acetobacterium dehalogenans*. *Eur. J. Biochem.* 253 (3), 706–711.
- Kiely, P.D., Regan, J.M., Logan, B.E., 2011. The electric picnic: synergistic requirements for exoelectrogenic microbial communities. *Curr. Opin. Biotechnol.* 22 (3), 378–385.
- Kuhn, E.P., Suflita, J.M., Rivera, M.D., Young, L.Y., 1989. Influence of alternate electron acceptors on the metabolic fate of hydroxybenzoate isomers in anoxic aquifer slurries. *Appl. Environ. Microbiol.* 55 (3), 590–598.
- Lalauette, E., Thammannagowda, S., Mohagheghi, A., Maness, P.-C., Logan, B.E., 2009. Hydrogen production from cellulose in a two-stage process combining fermentation and electrohydrogenesis. *Int. J. Hydrogen Energy* 34 (15), 6201–6210.
- Lewis, A.J., Ren, S., Ye, X., Kim, P., Labbe, N., Borole, A.P., 2015. Hydrogen production from switchgrass via an integrated pyrolysis–microbial electrolysis process. *Bioresour. Technol.* 195, 231–241.
- Logan, B., 2009. Exoelectrogenic bacteria that power microbial fuel cells. *Nat. Rev. Microbiol.* 7, 375–381.
- Logan, B.E., 2012. Essential data and techniques for conducting microbial fuel cell and other types of bioelectrochemical system experiments. *ChemSusChem* 5 (6), 988–994.
- Luo, H., Liu, G., Zhang, R., Jin, S., 2009. Phenol degradation in microbial fuel cells. *Chem. Eng. J.* 147 (2–3), 259–264.
- Madigan, M.T., Martinko, J.M., Dunlap, P.V., Clark, D.P., 2009. *Brock Biology of Microorganisms*. Pearson Benjamin Cummings, San Francisco, CA.
- Marone, A., Carmona-Martinez, A.A., Sire, Y., Meudec, E., Steyer, J.P., Bernet, N., Trably, E., 2016. Bioelectrochemical treatment of table olive brine processing wastewater for biogas production and phenolic compounds removal. *Water Res.* 100, 316–325.
- Mills, T.Y., Sandoval, N.R., Gill, R.T., 2009. Cellulosic hydrolyzate toxicity and tolerance mechanisms in *Escherichia coli*. *Biotechnol. Biofuel.* 2 (1), 1–11.
- Monlau, F., Sambusiti, C., Barakat, A., Quémener, M., Trably, E., Steyer, J.P., Carrère, H., 2014. Do furanic and phenolic compounds of lignocellulosic and algae biomass hydrolyzate inhibit anaerobic mixed cultures? A comprehensive review. *Biotechnol. Adv.* 32 (5), 934–951.
- Okutman Tas, D., Pavlostathis, S.G., 2008. Effect of nitrate reduction on the microbial reductive transformation of pentachloronitrobenzene. *Environ. Sci. Technol.* 42 (9), 3234–3240.
- Parameswaran, P., Zhang, H., Torres, C.I., Rittmann, B.E., Krajmalnik-Brown, R., 2010. Microbial community structure in a biofilm anode fed with a fermentable substrate: the significance of hydrogen scavengers. *Biotechnol. Bioeng.* 105 (1), 69–78.
- Ren, S., Ye, X.P., Borole, A.P., Kim, P., Labbé, N., 2016. Analysis of switchgrass-derived

- bio-oil and associated aqueous phase generated in a semi-pilot scale auger pyrolyzer. *J. Anal. Appl. Pyrolysis* 119, 97–103.
- Ren, Z., Ward, T.E., Regan, J.M., 2007. Electricity production from cellulose in a microbial fuel cell using a defined binary culture. *Environ. Sci. Technol.* 41 (13), 4781–4786.
- Rice, E.W., Eaton, A.D., Baird, R.B., 2012. Standard Methods for the Examination of Water and Wastewater APHA. AWWA, WEF, Washington, DC.
- Schie, P.M.v., Young, L.Y., 2000. Biodegradation of phenol: mechanisms and applications. *Bioremed. J.* 4 (1), 1–18.
- Schink, B., Philipp, B., Müller, J., 2000. Anaerobic degradation of phenolic compounds. *Naturwissenschaften* 87 (1), 12–23.
- Song, T.-s., Wu, X.-y., Zhou, C.C., 2014. Effect of different acclimation methods on the performance of microbial fuel cells using phenol as substrate. *Bioprocess Biosyst. Eng.* 37 (2), 133–138.
- Thygesen, A., Marzorati, M., Boon, N., Thomsen, A.B., Verstraete, W., 2011. Upgrading of straw hydrolysate for production of hydrogen and phenols in a microbial electrolysis cell (MEC). *Appl. Microbiol. Biotechnol.* 89 (3), 855–865.
- Tschech, A., Schink, B., 1986. Fermentative degradation of monohydroxybenzoates by defined syntrophic cocultures. *Arch. Microbiol.* 145 (4), 396–402.
- Tschech, A., Fuchs, G., 1989. Anaerobic degradation of phenol via carboxylation to 4-hydroxybenzoate: *In vitro* study of isotope exchange between $^{14}\text{CO}_2$ and 4-hydroxybenzoate. *Arch. Microbiol.* 152 (6), 594–599.
- van Schie, P.M., Young, L.Y., 1998. Isolation and characterization of phenol-degrading denitrifying bacteria. *Appl. Environ. Microbiol.* 64 (7), 2432–2438.
- Wang, H., Ren, Z.J., 2013. A comprehensive review of microbial electrochemical systems as a platform technology. *Biotechnol. Adv.* 31 (8), 1796–1807.
- Yaws, C.L., 2003. Yaws' Handbook of Thermodynamic and Physical Properties of Chemical Compounds. Elsevier/Knovel eBook.
- Zeng, X., Borole, A.P., Pavlostathis, S.G., 2015. Biotransformation of furanic and phenolic compounds with hydrogen gas production in a microbial electrolysis cell. *Environ. Sci. Technol.* 49 (22), 13667–13675.
- Zeng, X., Borole, A.P., Pavlostathis, S.G., 2016a. Performance evaluation of a continuous-flow bioanode microbial electrolysis cell fed with furanic and phenolic compounds. *RSC Adv.* 6, 65563–65571.
- Zeng, X., Borole, A.P., Pavlostathis, S.G., 2016b. Inhibitory effect of furanic and phenolic compounds on exoelectrogenesis in a microbial electrolysis cell bioanode. *Environ. Sci. Technol.* <http://dx.doi.org/10.1021/acs.est.6b01505>.
- Zhang, X., Wiegel, J., 1990. Isolation and partial characterization of a *Clostridium* species transforming *para*-hydroxybenzoate and 3,4-dihydroxybenzoate and producing phenols as the final transformation products. *Microb. Ecol.* 20 (1), 103–121.
- Zhang, X., He, W., Ren, L., Stager, J., Evans, P.J., Logan, B.E., 2015. COD removal characteristics in air-cathode microbial fuel cells. *Bioresour. Technol.* 176, 23–31.
- Zhang, Y., Angelidaki, I., 2014. Microbial electrolysis cells turning to be versatile technology: recent advances and future challenges. *Water Res.* 56, 11–25.